electronics

MDPI

Article

Magnetic-Free Nonreciprocal Multifunction Device Based on Switched Delay Lines

Fengchuan Wu, Yuejun Zheng and Yunqi Fu *

College of Electronic Science and Technology, National University of Defense Technology, Changsha 410073, China

* Correspondence: yunqifu@nudt.edu.cn

Received: 10 July 2019; Accepted: 1 August 2019; Published: 3 August 2019

Abstract: A magnetic-free multifunction nonreciprocal device based on switched delay lines (SDLs) has been proposed in this paper. It is constructed with two double balanced gyrators (DBGs) and four baluns, each pair of differential ports of the balun connect the ports at the same orientation of the two DBGs, respectively. Due to the asymmetry of the clock control signals acting on the switches, the time reversal symmetry of the transmission line between the Gilbert quad-switch-sets (GQSS) can be broken to achieve non-reciprocity. It can be used as a circulator, gyrator, or isolator by setting different control signals. The device has infinite working bandwidth in theory based on the SDLs. Common mode interference can be better suppressed by using differential transmission structures. Moreover, power capacity can be improved compared to the previous work. Then, experiments have been done to verify the device as a circulator. Broadband property and the anti-interference property have been verified.

Keywords: anti-interference; circulator; gyrator; isolator; magnetic-free; multifunction; nonreciprocal; power capacity; switched delay lines; ultra-broadband

1. Introduction

In the future, wireless cellular network communication and WIFI will be further improved, the integrated full-duplex system is expected to improve the channel capacity or communication speed of wireless cellular networks and WIFI. Circulator and isolator, as full-duplex or decoupling devices between transmitter and receiver, to avoid self-interference, play an irreplaceable role in duplex communication systems. The main feature of circulators and isolators are their nonreciprocity. Conventional nonreciprocal devices usually use magnetic materials such as ferrites [1,2] to achieve non-reciprocal property. However, the ferrite-based nonreciprocal devices are quite bulky and difficult to be integrated, which limits its further miniaturization. Moreover, non-reciprocal is exceptionally strong in structures with near-zero parameters, which is expected to be used to design nonreciprocal devices [3,4]. However, it has not been fully carried out and explored. So, several magnetic-free devices have been proposed to realize integration of nonreciprocal devices [5–17].

For magnetic-free nonreciprocal devices, there are several ways to realize them. Reciprocity can be broken with active transistors, either in discrete circuits or integrated circuits [5,6]. However, the use of active transistors severely limits the linearity and noise performance. Reciprocity can also be broken using nonlinearities [7]. However, nonlinear devices typically exhibit non-reciprocity over a limited range of signal powers, and have limited bandwidth, precluding their application in scenarios where linearity to the desired signal is required. Parametrically modulated coupled-resonator loops have been proposed to construct the magnetic-free circulators with subwavelength dimensions [8,9]. However, they will produce intermodulation and harmonic products, and the working bandwidth is limited. At microwave frequencies, permittivity modulation is typically achieved using varactors that exhibit a

limited maximum-to-minimum capacitance ratio ranging from 2 to 4, thus leading to large devices. Shihan Qin et al. proposed the time varying transmission lines (TVTL) to construct magnetic-free nonreciprocal devices [8], where the distributed capacitive mixers are used to the TVTL. When the direction of the transmission signal is the same as the carrier's, the transmission signal will mix with the carrier. However, if the transmission signal and the carries are in opposite directions, they will not mix up. So, the TVTL can be used as a frequency conversion isolator or a circulator. However, a lengthy circuit is needed to realize the spectrum shift. Reiskarimian et al. proposed a staggered commutation theory to realize magnetic-free circulators, and fabricated an integrated circulator for the first time [11,12]. However, this design has limited power handling ability and is hard to work at millimeterwave band. Nagulu et al. proposed a new kind of TVTL which is called SDL, to realize magnetic-free circulator working at millimeterwave band [13–15]. However, the working band of the circulator is limited. Ultra-wideband circulators have been proposed in previous work based on the balanced gyrator (BG) and double balanced gyrator (DBG), respectively [15]. Adjusting the clock control signal, the DBG can be used as a frequency conversion isolator [15]. However, the anti-interference performance and power capacity of the ultra-broadband circulator based on the DBG are limited. Also, the bandwidth of the frequency conversion isolator is limited.

In this paper, a magnetic-free nonreciprocal multifunction device, which can be used as a circulator, gyrator, or isolator by changing the clock control signals, is proposed. Besides, the anti-interference performance and power capacity of the device can be improved at the same time by using differential transmission line segments. It also has infinite working bandwidth in theory. The properties mentioned above can be realized at the same time in this work. This paper is organized as follows:

Section 2 introduces the principle of the magnetic-free nonreciprocal device as a gyrator, circulator, and isolator. Section 3 presents the simulation verification of the device as a circulator and isolator, and the anti-interference performance of the device is also verified. Section 4 presents the experiment of the device as a circulator. Finally, a conclusion is made in Section 5.

2. Principle of the Device

The schematic of the proposed device is shown in Figure 1, which consists of two DBGs and four baluns. Each pair of differential ports of the balun connect the ports at the same orientation of the two DBGs, respectively. The GQSS in the DBG are controlled by the clock signals. The switch keeps on (off) when at a high (low) level of the control signal acting on the switches.

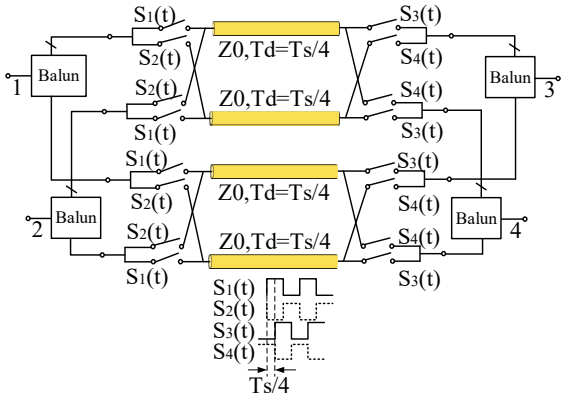

Figure 1. Schematic of the proposed magnetic-free device.

2.1. Gyrator

For the gyrator, keeping the clock control signal is shown in Figure 1. Regard port 1(2) and port 3(4) as port 1+ (1−) and port 2+ (2−), respectively. The device can be regarded as a two-port network.

When the transmission signals are input from port 1 and port 3, the output signals at port 2 and port 4 can be written as:

$$\begin{aligned} V_2^{\pm}(t) &= V_1^{\pm}(t-\tfrac{T_s}{4})\left[S_1(t-\tfrac{T_s}{4})\times S_3(t)+S_2(t-\tfrac{T_s}{4})\times S_4(t)\right]+V_1^{\mp}(t-\tfrac{T_s}{4})\left[S_1(t-\tfrac{T_s}{4})\times S_4(t)+S_2(t-\tfrac{T_s}{4})\times S_3(t)\right] \\ &= V_1^{\pm}(t-\tfrac{T_s}{4})\times S_1(t-\tfrac{T_s}{4})\times S_3(t)+V_1^{\pm}(t-\tfrac{T_s}{4})\times S_2(t-\tfrac{T_s}{4})\times S_4(t) \\ &= V_1^{\pm}(t-\tfrac{T_s}{4}), \end{aligned} \tag{1}$$

Where $V_1^{\pm}(t)$, $V_2^{\pm}(t)$ are the transmission signal at port 1(2) and port 3(4), respectively. *Sn(t)* (n = 1, 2, 3, 4) is the clock control signal. *Ts* is the period of the clock signals. The clock signals of the right switches are delayed with respect to the left switches by a value which equals to the propagation delay of the delay line *Ts/4*.

When the transmission signals are input from port 2 and port 4, the output signals at port 1 and port 3 can be written as:

$$\begin{aligned} V_1^{\pm}(t) &= V_2^{\pm}(t-\tfrac{T_s}{4})\left[S_3(t-\tfrac{T_s}{4})\times S_1(t)+S_4(t-\tfrac{T_s}{4})\times S_2(t)\right]+V_2^{\mp}(t-\tfrac{T_s}{4})\left[S_4(t-\tfrac{T_s}{4})\times S_1(t)+S_3(t-\tfrac{T_s}{4})\times S_2(t)\right] \\ &= V_2^{\mp}(t-\tfrac{T_s}{4})\times S_4(t-\tfrac{T_s}{4})\times S_1(t)+V_2^{\mp}(t-\tfrac{T_s}{4})\times S_3(t-\tfrac{T_s}{4})\times S_2(t) \\ &= V_2^{\mp}(t-\tfrac{T_s}{4}) \end{aligned} \tag{2}$$

The scattering parameter matrix of DBG can be written as:

$$S=\begin{pmatrix} 0 & -e^{-j\omega\frac{T_s}{4}} \\ e^{-j\omega\frac{T_s}{4}} & 0 \end{pmatrix}, \tag{3}$$

From Equation (2), the nonreciprocal phase property of the gyrator is also frequency independent. Transmission procession of the signals in the device as a circulator or gyrator is shown in Figure 2. When signals are input from port 1 (1+) and port 2 (1−), they will be transmitted to port 3 (1+) and port 4 (1−); when signals are input from port 3 (2+) and port 4 (2−), they will be transmitted to port 2 (1−) and port 1 (1+).

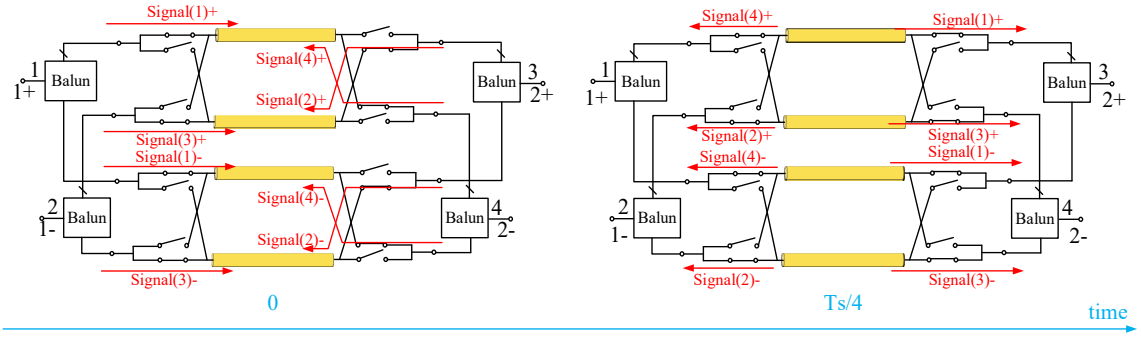

Figure 2. Transmission procession of the signals in the gyrator (circulator).

2.2. Circulator

As for the circulator, the DBG proposed in previous work can be considered as an ultra-broadband single-ended four-port circulators, which has been verified by R. Lu et al. [16]. However, it has limited power capacity and anti-interference performance by using single-ended transmission structures. Assuming the DBG is a well-matched four-port network without considering the bandwidth and dispersion of the transmission line, the scattering parameter matrix can be written as:

$$S=\begin{pmatrix} 0 & 0 & 0 & e^{-j\omega\frac{T_s}{4}} \\ e^{-j\omega\frac{T_s}{4}} & 0 & 0 & 0 \\ 0 & e^{-j\omega\frac{T_s}{4}} & 0 & 0 \\ 0 & 0 & e^{-j\omega\frac{T_s}{4}} & 0 \end{pmatrix}, \tag{4}$$

Ts is the period of the clock signals. The clock signals of the right switches are delayed with respect to the left switches by a value which equals to the propagation delay of the transmission line *Ts*/4. And ω represents the transmission frequency. For the differential transmission circulator (DTC), combine the two DBGs with four frequency-independent baluns shown in Figure 1. The scattering parameter matrix can also be written as Equation (4). The nonreciprocal property is frequency independent.

2.3. Isolator

For lower DBG structures in the DTC, setting S1(t), S2(t), S3(t), S4(t) as DC voltages. S1(t) and S3(t) acting on the lower DBG are at the high level to keep the switches on; S2(t) and S4(t) acting on the lower DBG are at the low level to keep the switches off. Thus, the lower DBG can be regarded as a pair of reciprocal transmission line segments. The clock control signals acting on the upper DBG keep the same as shown in Figure 1. Thus, the device can be regarded as a magnetic-free isolator called a differential transmission isolator (DTI), which is similar in the previous work [17]. However, the Wilkinson power splitters (combiners) are replaced by the baluns in this paper, which can suppress the common mode signals. So, the reverse transmission signals can be designed as the common signals to be suppressed by the baluns.

The transmission process of the signals is shown in Figure 3. When a pair of differential signals input from port 1+ and 1−, the baluns divide the two sets of signals into four sets of signals with equivalent power. Then, the signals will be combined at the baluns with antiphase at port 2+ and 2− respectively. Finally, the signals will be output from port 2+ and 2−.

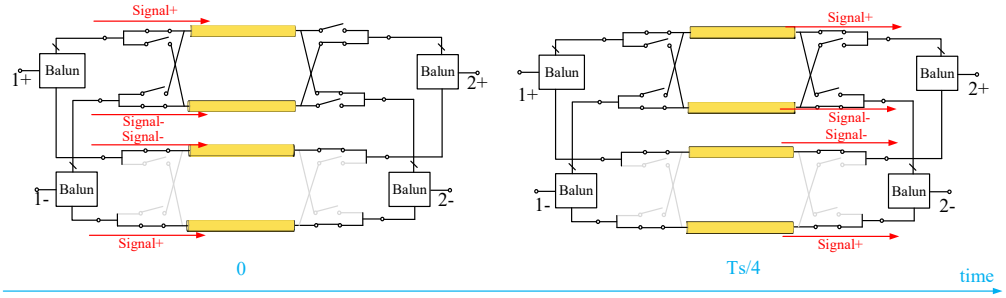

(a)

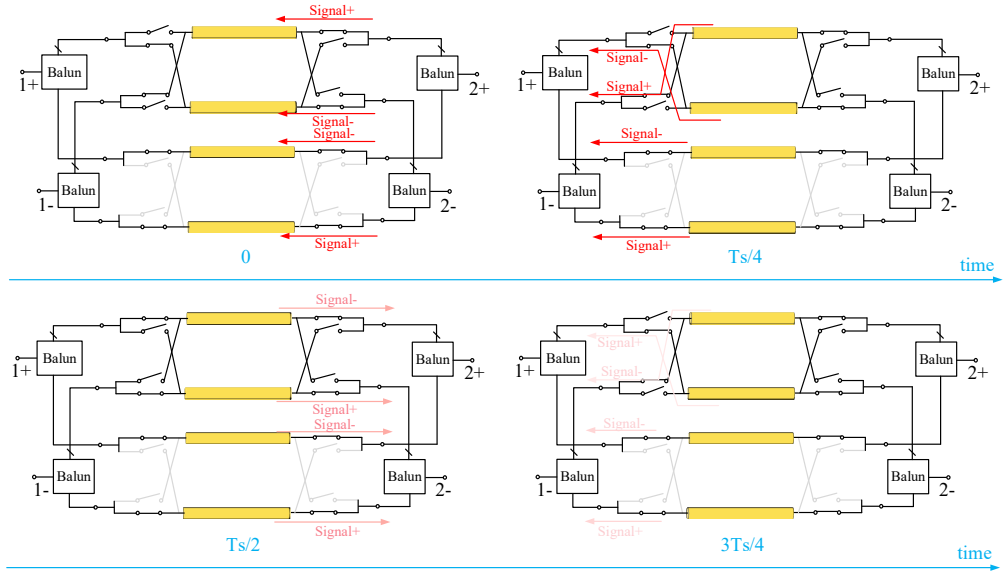

(b)

Figure 3. Transmission procession of the signals in the isolator. (**a**) Input from port 1+ (1−); (**b**) Input from port 2+ (2−).

When a pair of differential signals are input from port 2+ and 2−, respectively, the signals will be combined in phase at the baluns at port 1+ and 1-, respectively. So, the signals can be regarded as common mode signals. The common mode signals will be suppressed significantly by the baluns. Assume that small parts of signals are reflected back to the baluns at port 2+ and 2−, the signals will be combined in phase at the baluns twice. So, the reverse signals can be further suppressed. And the remained signals will be reflected back to the baluns at port 1+ and 1−. Finally, the remained signals will be output from port 1+ and 1−. However, the output signals have been suppressed significantly.

3. Simulation Verification of the Device

The harmonic balance module in the Keysight Advanced Design System (ADS) simulation software was used to get the spectrum results of the device, to verify ultra-broadband properties. Assuming all the transmission line segments with no dispersion and have a delay time of Ts/4 = 0.5 ns. The phase relationships between the clock signals are the same as shown in Figure 1. The frequency range of the input signal is from 0.1 to 1 GHz, with a step size of 0.1 GHz. The input power is set as 10 dBm.

3.1. Circulator

For the DTC, the results shown in Figure 4 indicate that the transmission direction of the DTC is 1-2-3-4-1. Throughout the simulation band, the insertion loss is lower than 0.1 dB along the transmission direction. The reverse isolation is higher than 50 dB. And it is increased gradually with the frequency. The second isolated port has isolation higher than 80 dB throughout the simulation band.

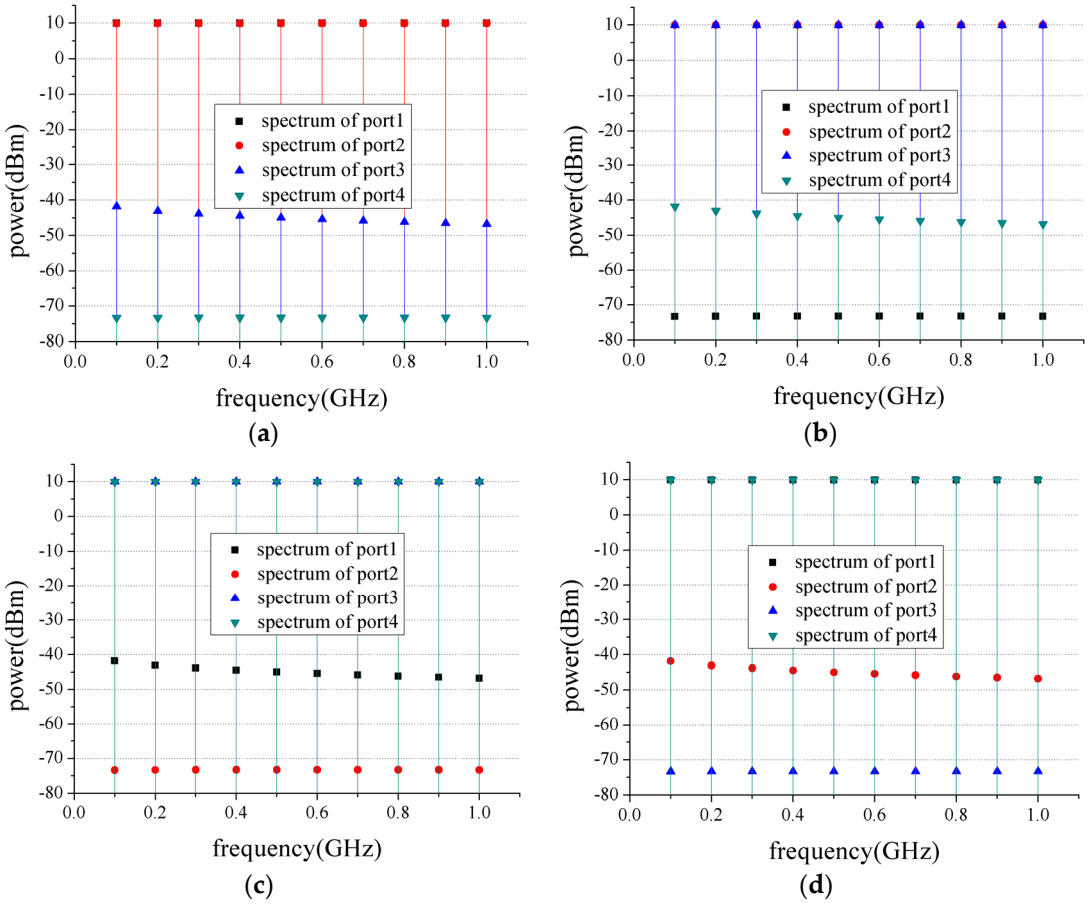

Figure 4. Simulation results of the DTC. (**a**) Input from port 1; (**b**) Input from port 2; (**c**) Input from port 3; (**d**) Input from port 4.

When the device is used as a 4-port circulator, the transmitter, receiver, and antenna can be connected to port 1, port 2, and port 3, respectively; the matching load is expected to be connected to port 4 so that the transmitter and receiver have enough isolation.

In order to verify the advantage of the DTC in anti-interference performance, two noise modules were built up, shown in Figure 5. As the noise is usually generated from a single noise source, a common mode interference is added at port 1 of the DTC, and a single noise source is added at port 1 of the single-ended transmission circulator (STC), which is constructed by a DBG.

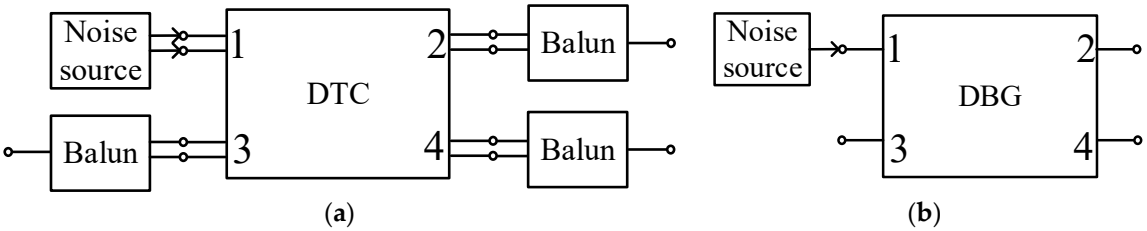

Figure 5. Noise module of the circulators. (**a**) Noise module of the DTC; (**b**) Noise module of the STC.

The power of the noise interference is set as 10 dBm. The frequency range of the common mode interference is from 0.1 to 1 GHz, with a step size of 0.1 GHz. From the results shown in Figure 6a. The common mode interference can be suppressed over 60 dB throughout the simulation band, which is similar to the situation as a gyrator. As for the STC, the results are shown in Figure 6b which indicate that the interference cannot be suppressed. Thus, the anti-interference performance can be improved compared to the STC.

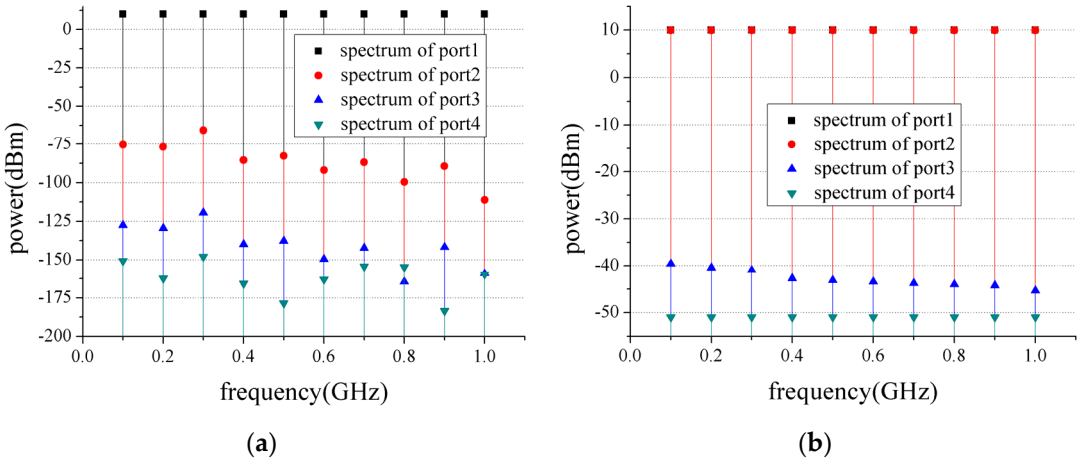

Figure 6. Spectrum simulation results of the DTC and the STC. (**a**) DTC; (**b**) STC.

Besides, the DTC has a higher power capacity than the STC. By using ultra-broadband baluns, which can be regarded as power splitters (combiners), the DTC can theoretically raise 3 dB power capacity compared to the STC. Thus, the circulator can be better protected.

3.2. Isolator

For the isolator, spectrum simulations have been done to verify it, which have the same simulation settings as mentioned above. The simulation results are shown in Figure 7. Throughout the simulation band, the insertion loss is lower than 0.1 dB along the transmission direction. The reverse isolation is higher than 70 dB, which is increased gradually with the frequency. So, it can be used as an ultra-broadband isolator.

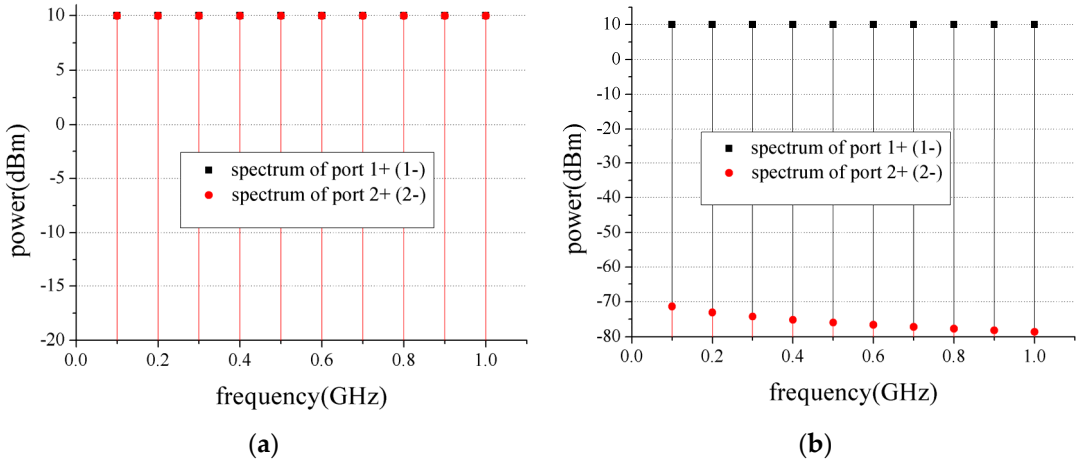

Figure 7. Spectrum simulation results of the isolator. (**a**) Input from port 1+ (1−); (**b**) Input from port 2+ (2−).

A common mode noise source has been added to the isolator to verify the anti-interference performance. The noise module is shown in Figure 8. Two situations are considered: (1) The common mode noise is input from port 1+ (2+) and 1− (2−) of the isolator, respectively. (2) The common mode noise is input from one side of the two reciprocal transmission line segments and DBG, respectively.

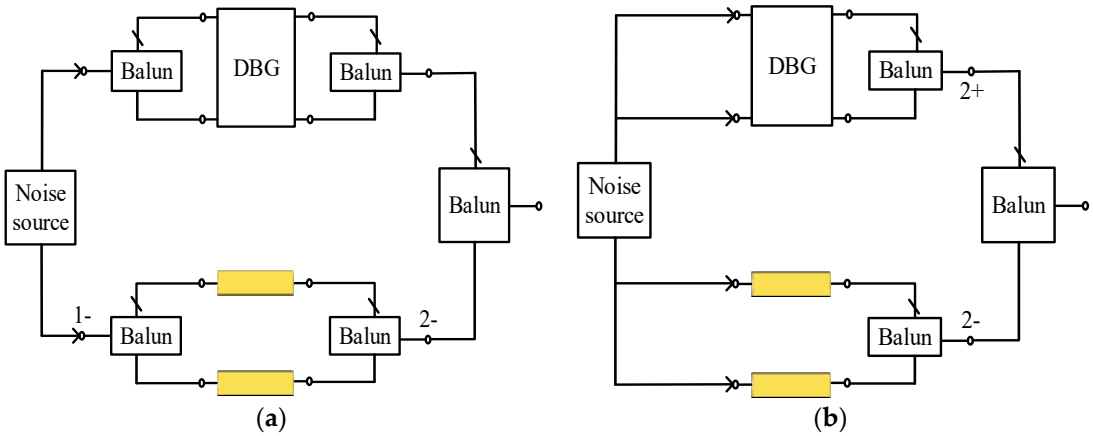

Figure 8. Noise module of the isolator. (**a**) Input from port 1+ and 1−; (**b**) Input from the DBG and two reciprocal transmission line segments, respectively.

The simulation results are shown in Figure 9. The spectrum results show that the isolator has a significant suppression of the common mode signals over the entire simulation band in these two situations. The suppression of the common mode signals is higher than 70 dB when the common mode noise is input from port 1+ and port 1− throughout the simulation band. The suppression is higher than 75 dB when it is input from the DBG and two reciprocal transmission lines throughout the simulation band. The average suppression of the situation (2) is about 40 dB higher than the average suppression of the situation (1).

In summary, the device is easy to be integrated without the use of ferrite materials. Besides, according to the simulation results, the device has ultra-broadband working bandwidth, well anti-interference, and high isolation for the reverse signal. However, the device needs very accurate clock control signals and the delay lines with precise length to ensure the performances.

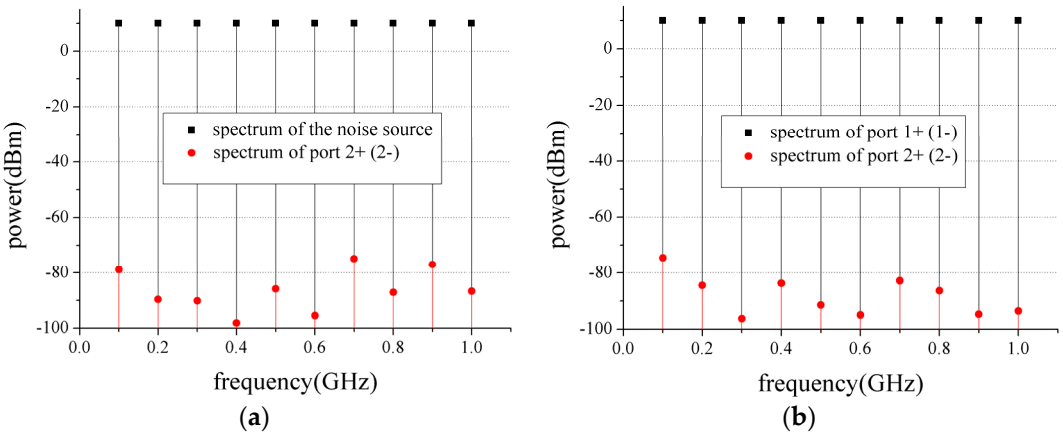

Figure 9. The spectrum of the common mode noise of the isolator. (**a**) Input from port 1+ and 1−; (**b**) Input from the DBG and two reciprocal transmission line segments, respectively.

4. The Experiments of the Magnetic-Free Nonreciprocal Device

A prototype was made to verify the broadband and anti-interference properties, as shown in Figure 10, which is also inspired by the previous work [9]. In this design, the GQSS in the DBG were made of 1.6-mm FR-4 printed circuit broad (PCB), and four Minicircuits' single-pole-double-throw (SPDT) switches. The typical transition time of the swithes is 4 ns. The balun was made of 1.6-mm FR-4 PCB and a Minicircuits' ADTL1-12+ RF transformer. The working band of the balun is 20~1200 MHz. The transmission line segments were realized by four 7-meter coaxial cables. The matching loads were realized by 50Ω end caps. The four clock signals were generated by four synchronized Tektronix AFG31023C signal generators, and the frequency of the clock signals in this design was chosen as 6.9 MHz. The N5244A network analyzer is used to measure out the S parameters. The insertion loss of the coaxial cable is increased with frequency. Therefore, the signals higher than 1.2 GHz is not obtained. Moreover, limited by the bandwidth of the baluns, the measurement band is chosen as 10~1200 MHz.

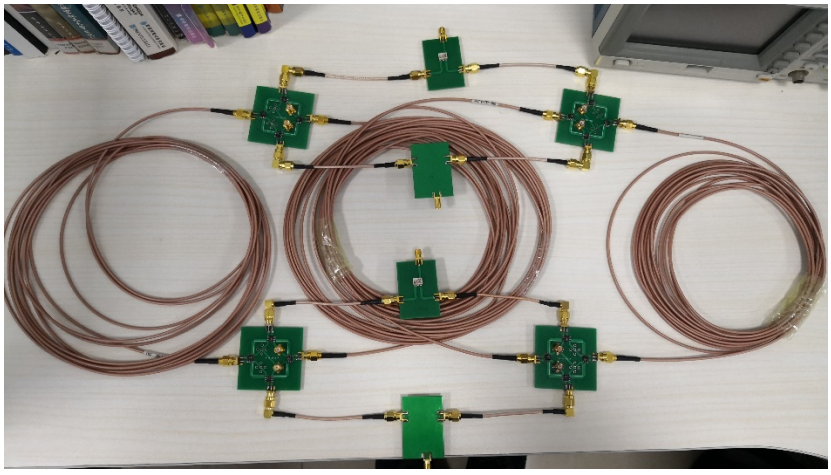

Figure 10. The prototype of the magnetic-free nonreciprocal device.

The measured S-parameters are shown in Figure 11. From the results, the transmission direction of the circulator is 1-2-3-4-1. The results show that the return loss is higher than 10 dB throughout the band of 200~1200 MHz. So, the circulator has broadband property. The minimum insertion loss of the circulator is about 7 dB. It is generally increased with the frequency. The delay error of the transmission line segments and duty cycle error of the clock signals are the main reason that increase the insertion loss. Besides, the transmission line segments and the baluns also influence the insertion loss. The reverse isolation is higher than 36 dB throughout the measurement band. The average

deviation of the simulation and the experiment is 25 dB within the band of 0~1000 MHz, which is caused by the error of the clock control signals and the amplitude and phase imbalance of the baluns.

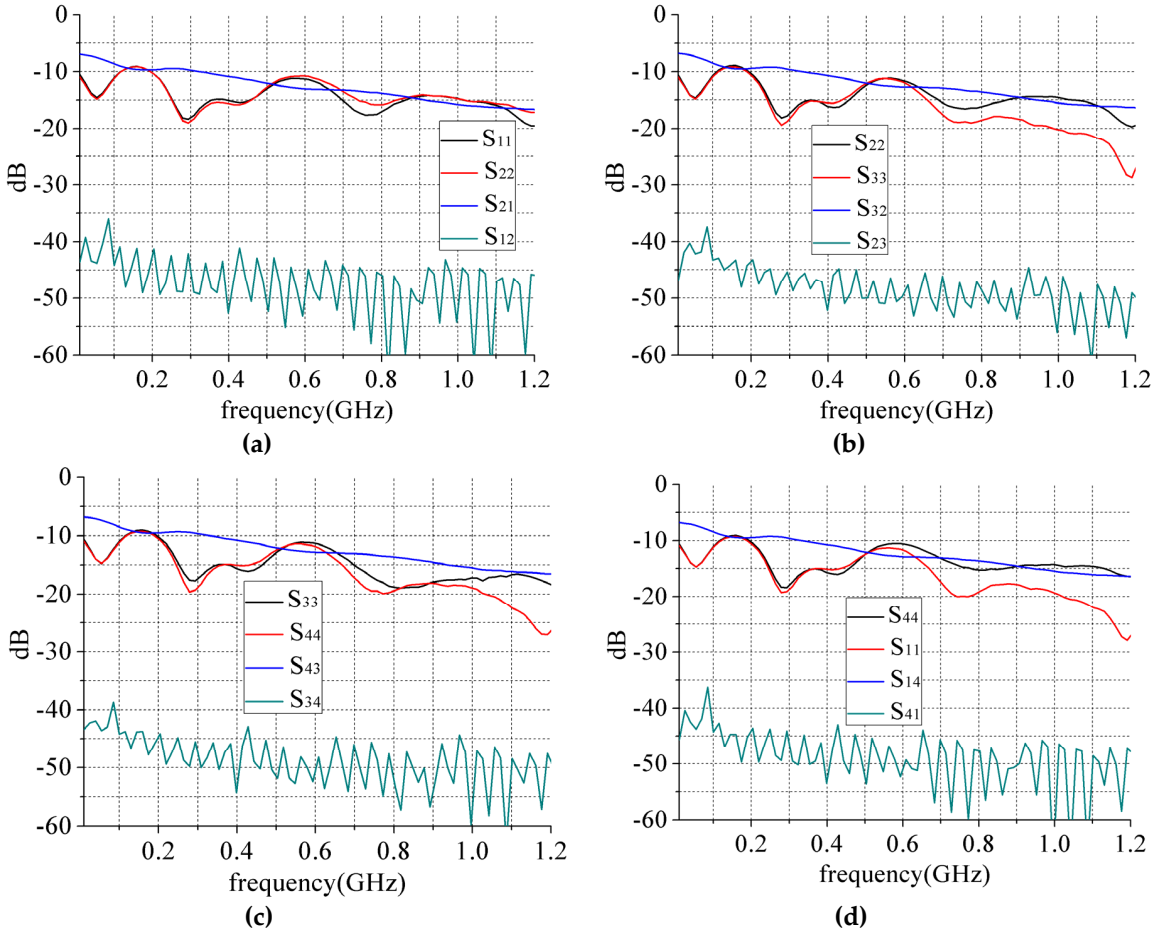

Figure 11. The measured S parameters of the magnetic-free nonreciprocal device. (**a**) Port 1 and port 2. (**b**) Port 1 and port 2. (**c**) Port 1 and port 2. (**d**) Port 1 and port 2.

The broadband balun chose in this paper is about −10 dB throughout the band of 20~1200 MHz. Also, due to the phase and amplitude imbalance of the baluns, the return loss of the structure is not high. The return loss of the DTC can be increased by designing the balun, which is well-matched and has low amplitude and phase unbalance in the broadband range.

The delay error of the coaxial cables and the duty cycle error of the clock signals have significate impacts on the insertion loss of the DTC. The insertion loss can be reduced by using advanced integration technology to make subnanosecond switches, precise delay lines, and produce high quality clock signals.

To verify the anti-interference performance of the circulator, replace one balun in the circulator with a Wilkinson power splitter to generate a pair of co-phase equal amplitude signals as the common mode signal. The prototype is shown in Figure 12. The working band of the Wilkinson power splitter is 380~2500 MHz. Two ports with baluns in the circulator are connected with two 50Ω end caps respectively. The other two ports are connected with the PNA network analyzer. The measurement results are shown in Figure 13. The result shows that the suppression of the common mode signal is higher than 40 dB throughout the band of 20~1200 MHz, which indicates that the circulator can effectively suppress common mode interference within the broadband range. The average deviation of the simulation and the experiment is 44 dB within the band of 400~1000 MHz.

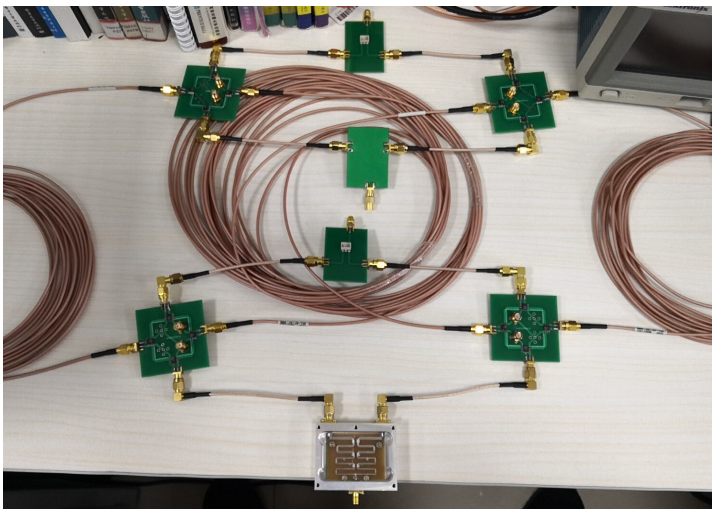

Figure 12. Anti-interference testing module.

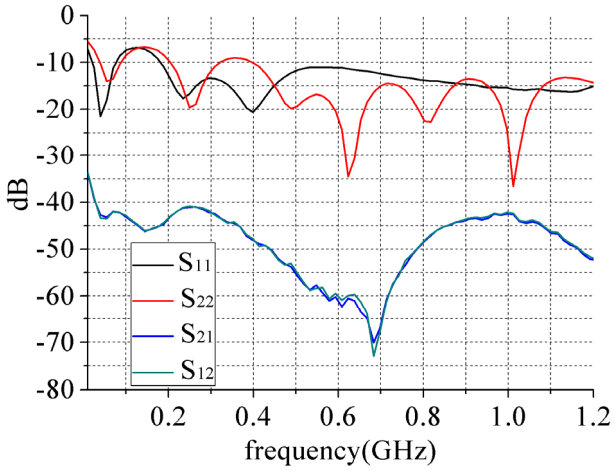

Figure 13. The measured S parameters of the anti-interference testing module.

With the limitation of the experimental conditions, the delay error of the transmission line segments and duty cycle error of the clock signals cannot be avoided. The two kinds of errors have significant impacts on the insertion loss. The signals pass through the DBG, and reciprocal transmission line segments, respectively, are hard to be combined with equal amplitude at the baluns. As a result, the magnetic-free nonreciprocal device as an isolator is difficult to be verified by using a PCB circuit. The experiment of the isolator is expected to be realized in the future by using precise clock signals and advanced processing technology in the integration circuit.

5. Conclusions

A magnetic-free device has been designed in this paper, which can be used as a gyrator, circulator, or isolator by only adjusting the clock control signals to achieve multifunctional nonreciprocal features. Simulation works have been done to verify the ultra-broadband property of the device. Besides, the anti-interference performance of the device as a circulator and isolator is also verified. The common mode noise can be significantly suppressed by using differential transmission structures. Moreover, the power capacity can be improved by 3 dB theoretically compared to the previous work [15]. The magnetic-free nonreciprocal device as a broadband circulator has been verified by the experiment. Besides, broadband anti-interference property is also verified. The properties of the magnetic-free circulators and isolators based on SDL are displayed in Tables 1 and 2, respectively. From Table 1, compared to the ultra-broadband circulator (UBC) and high linearity circulator (HLC)

in [15], and single-ended transmission circulator (STC) in [16], the DTC proposed in this paper has ultra-broadband, well anti-interference performances at the same time. Besides, the DTC has the largest power capacity. From Table 2, the DTI proposed in this paper has both ultra-broadband and well anti-interference performances. Moreover, the DTI has the largest power capacity compared to the other two isolators shown in Table 2. The delay error of the clock signals, delay lines, and the duty cycle error of the clock signals, which have significant impacts on the insertion loss, can be reduced by using precise clock signals and advanced processing technology in the integration circuit. Moreover, exploration of new metamaterials can be considered to improve magnetic-free nonreciprocal devices.

Table 1. The properties of the device as a circulator.

	DTC in this Paper	**UBC in [15]**	**HLC in [15]**	**STC in [16]**
Bandwidth	Ultra-Broadband	Ultra-Broadband	Limited	Ultra-Broadband
Anti-interference performance	Well	Limited	Well	Limited
Power capacity	Largest	Smallest	Medium	Smallest

Table 2. The properties of the device as an isolator.

	DTI in this paper	**UDI in [15]**	**FCI in [15]**
Bandwidth	Ultra-Broadband	Ultra-Broadband	Limited
Anti-interference performance	Well	Limited	Well
Power capacity	Largest	Smallest	Medium

Author Contributions: Methodology and original draft preparation, F.W.; writing—review and editing, Y.Z. and Y.F.; writing—review and editing, supervision, Y.F.

Funding: This research received no external funding.

Acknowledgments: The authors would like to thank Nagulu and Krishnaswamy for valuable discussions.

Conflicts of Interest: The authors declare no conflict of interest.

References

1. Dong, H.; Smith, J.R.; Young, J.L. A Wide-Band, High Isolation UHF Lumped-Element Ferrite Circulator. *IEEE Microw. Wirel. Compon. Lett.* **2013**, *23*, 294–296. [CrossRef]
2. Zeng, L.; Tong, C.E.; Blundell, R.; Grimes, P.K.; Paine, S.N. A Low-Loss Edge-Mode Isolator With Improved Bandwidth for Cryogenic Operation. *IEEE Trans. Microw. Theory Tech.* **2018**, *66*, 1–7. [CrossRef]
3. Liberal, I.; Engheta, N. Erratum: Near-zero refractive index photonics. *Nat. Photonics* **2017**, *11*, 264. [CrossRef]
4. Pacheco-Peña, V.; Beruete, M.; Rodríguez-Ulibarri, P.; Engheta, N. On the performance of an ENZ-based sensor using transmission line theory and effective medium approach. *New J. Phys.* **2019**, *21*, 043056. [CrossRef]
5. Wang, S.; Lee, C.H.; Wu, Y.B. Fully integrated 10-GHz active circulator and quasi-circulator using bridged-T networks in standard CMOS. *IEEE Trans. Very Large Scale Integr. Syst.* **2016**, *24*, 3184–3192. [CrossRef]
6. Mung, S.W.Y.; Chan, W.S. Active Three-Way Circulator Using Transistor Feedback Network. *IEEE Microw. Wirel. Compon. Lett.* **2017**, *27*, 476–478. [CrossRef]
7. Popa, B.I.; Cummer, S.A. Nonreciprocal active metamaterials. *Phys. Rev. B* **2012**, *85*, 205101. [CrossRef]
8. Estep, N.A.; Sounas, D.L.; Alu, A. Magnetless Microwave Circulators Based on Spatiotemporally Modulated Rings of Coupled Resonators. *IEEE Trans. Microw. Theory Tech.* **2016**, *64*, 502–518. [CrossRef]
9. Kord, A.; Sounas, D.L.; Alu, A. Pseudo-Linear Time-Invariant Magnetless Circulators Based on Differential Spatiotemporal Modulation of Resonant Junctions. *IEEE Trans. Microw. Theory Tech.* **2018**, *66*, 2731–2745. [CrossRef]
10. Qin, S.; Xu, Q.; Wang, Y.E. Nonreciprocal Components With Distributedly Modulated Capacitors. *IEEE Trans. Microw. Theory Tech.* **2014**, *62*, 2260–2272. [CrossRef]

11. Reiskarimian, N.; Zhou, J.; Chuang, T.H.; Krishnaswamy, H. Analysis and Design of Two-Port N-Path Band-Pass Filters with Embedded Phase Shifting. Circuits and Systems II: Express Briefs. *IEEE Trans.* **2016**, *63*, 728–732.
12. Reiskarimian, N.; Zhou, J.; Krishnaswamy, H. A CMOS Passive LPTV Nonmagnetic Circulator and Its Application in a Full-Duplex Receiver. *IEEE J. Solid State Circuits* **2017**, *52*, 1358–1372. [CrossRef]
13. Dinc, T.; Nagulu, A.; Krishnaswamy, H. A Millimeter-Wave Non-Magnetic Passive SOI CMOS Circulator Based on Spatio-Temporal Conductivity Modulation. *IEEE J. Solid State Circuits* **2017**, *52*, 3276–3292. [CrossRef]
14. Dinc, T.; Tymchenko, M.; Nagulu, A.; Sounas, D.; Alu, A.; Krishnaswamy, H. Synchronized conductivity modulation to realize broadband lossless magnetic-free non-reciprocity. *Nat. Commun.* **2017**, *8*, 795. [CrossRef] [PubMed]
15. Nagulu, A.; Dinc, T.; Xiao, Z.; Tymchenko, M.; Sounas, D.L.; Alù, A.; Krishnaswamy, H. Nonreciprocal Components Based on Switched Transmission Lines. *IEEE Trans. Microw. Theory Tech.* **2018**, *66*, 4706–4725.
16. Lu, R.; Krol, J.; Gao, L.; Gong, S. A Frequency Independent Framework for Synthesis of Programmable Non-reciprocal Networks. *Sci. Rep.* **2018**, *8*, 14655. [CrossRef] [PubMed]
17. Fengchuan, W.; Yuejun, Z.; Fang, Y.; Yunqi, F. Magnetic-Free Isolators Based on Time-Varying Transmission Lines. *Electronics* **2019**, *8*, 684.